J Clin Res Paramed Sci. 2022 June; 11(1):e124080. https://doi.org/10.5812/jcrps-124080.

Published online 2022 June 20. **Research Article**

In Vitro Studies and Evaluation of Antibacterial Properties of Biodegradable Bone Joints Based on PLA/PCL/HA

Farnaz Dehghani Firoozabadi [1], Ahmad Ramazani Saadatabadi [2,*] and Azadeh Asefnejad [1]

[1] Department of Biomedical Engineering , Science and Research Branch, Islamic Azad University , Tehran, Iran
[2] Department of Chemical and Petroleum Engineering, Sharif University of Technology, Tehran, Iran

[*] *Corresponding author*: Department of Chemical and Petroleum Engineering, Sharif University of Technology, Tehran, Iran. Email: ramazani@sharif.edu

Received 2022 March 14; **Revised** 2022 May 15; **Accepted** 2022 May 16.

Abstract

Background: Due to the history of using permanent implants and the ability of adaptations of polymers to physiological environments such as the body environment, the need to design a polymer implant with a new formulation for orthopedic applications was felt.

Methods: Polymer joints in this study were made by solvent casting method. The mechanical properties of the samples were investigated by bending tests, before and after immersion in simulated body fluid (SBF). Morphology of nanocomposites, bioactivity of samples and initiation of degradation process were performed by field emission scanning electron microscope (FESEM). Toxicity test was performed to evaluate the toxicity of nanocomposites. The antibacterial properties of the samples were investigated by examining the zone of inhibition and measuring the photometric concentration. Biodegradability test was performed to prove the biodegradability of polymer joints.

Results: It was found that the mechanical properties of nanostructures increased with the addition of nanoparticles. Also, the presence of oxide and graphene nanoparticles affected the antibacterial properties of the composite nanostructure. Immersion in SBF solution showed that the nanostructures were biodegradable and bioactive. The results of this study indicate that the optimal nanocomposite PLA-PCL-HA-1% ZNO-1% GR has a Young's modulus close to spongy bone and reduces the stress shielding phenomenon. The flexural Yang modulus of the PLA-PCL-HA nanocomposite was 2139.037 ± 381.312 MPa. The presence of zinc oxide and graphene nanoparticles increased the Young's modulus to 4363.636 ± 127.498 MPa. The optimal sample has the necessary lethality against two strains of gram-positive and gram-negative bacteria and due to its bioactivity is a suitable option for use in spongy bone tissue. In this study, the viability of fibroblast cells in the vicinity of the polymer matrix versus the optimal matrix increased from 22.14 ± 0.623 to 82.96 ± 1.101% after 72 hours.

Conclusions: Improving cell viability indicates a reduction in the optimal matrix toxicity compared to the polymer matrix.

Keywords: Antibacterial, Biodegradability, Hard Tissue, Nanocomposite, *Escherichia coli*, *Staphylococcus aureus*

1. Background

Bone tissue is one of the vital and multifunctional tissues of the body. Although one of the unique features of this tissue is its ability to self-repair large fractures and defects, sometimes the healing process performed by the body is not enough and surgical interventions are necessary. The best option for orthopedic surgery is to use an implant that can stimulate tissue to bone formation. It should also be a suitable option for the patient and in addition to creating a suitable substrate for bone repair and reconstruction, eliminate the patient's need for a second surgery to remove the implant (1). The need to build biocompatible and bioactive scaffolds that can accelerate the healing process of broken and damaged bones has been considered by tissue engineering and biomaterials. In tissue engineering, temporary 3D scaffolding plays an important role in improving the function of osteoblasts and guiding them to form new bone in various forms. A biodegradable scaffold with sufficient mechanical strength, with optimal structure and suitable degradation rate that can be replaced with newly formed bone is the most desirable (2). The materials used to make scaffolds in bone tissue engineering must be able to conduct bone so that the bone precursor cells can migrate to the scaffolds, differentiate, and eventually form new bone. Hence, the use of biomaterials and tissue engineering has greatly expanded in the last decade due to the increasing demand for tissues and artificial organs. Various types of biomedical materials, such as bioactive ce-

ramics and biodegradable polymers, have been designed and manufactured to meet the mechanical and biological properties required by tissues (3). Today, most bone grafts are permanent and therefore, after tissue repair, there is a need to remove the implant from the tissue. Due to the high Young's modulus of metal implants, the transfer of force from the implant to the tissue does not occur properly and therefore weakens the tissue around the implant and ultimately leads to implant loosening. This phenomenon occurs due to differences in bone and implant Young's modulus, which is called the stress shielding phenomenon (4). Therefore, the use of biodegradable materials that have a Young's modulus in the range of natural bone tissue has received much attention. Polylactic acid is a low molecular weight, biodegradable and biocompatible multifunctional polymer that has been used specifically for medical applications. However, due to its fragile structure, its application alone is not a suitable option for use in areas under load (5). Polycaprolactone (PCL) is a semi-crystalline biodegradable aliphatic polyester and undergoes hydrolytic degradation due to the sensitivity of its aliphatic ester bond to hydrolysis. Extensive in-body and out-of-body compatibility and efficacy studies have been performed on this polymer, which has led to the approval of a number of medical and pharmaceutical devices by the US Food and Drug Administration (6). PCL is currently considered as a soft and hard tissue compatible material including absorbable sutures, drug delivery system and bone graft alternatives. Applications of PCL may be limited because its degradation and adsorption kinetics are much slower than other aliphatic polyesters, but due to their hydrophobicity and high crystallization properties, PCL is currently being studied as a potential substrate for bone regeneration (7). Poor mechanical properties of PCL, depending on the preparation method and molecular weight, limit its use as a scaffold to replace hard tissue. Therefore, strategies to improve the mechanical performance of PCL-based scaffolds are needed (8). One possible strategy to increase the mechanical properties is to reinforce the PCL with rigid hydroxyapatite particles, which also improves the conductivity of the polymer. In addition, achieving good porosity is crucial for the success of these materials as scaffolding for orthopedic applications. A pilot study on HA in PCL scaffolds has shown that the presence of HA in PCL substrates increases the function and growth of osteoblast cells. It has also been shown that the adhesion of proteins and osteoblasts to nano-sized ceramic particles increases (9). Degradation of polylactic polymer in the body causes acidification of the surrounding tissue and leads to inflammatory responses. Adding hydroxyapatite can buffer acidic products (10). Graphene is a two-dimensional structure of a single layer of carbon honeycomb network. Graphene has become a unique material due to its excellent properties in electrical conductivity, thermal conductivity, mobility of carriers, optical conductivity and mechanical properties. Graphene is a monolayer aromatic carbon which, due to its extremely inherent properties, is a suitable candidate for improving mechanical, optical, electrical and thermal conductivity properties. With 1 Tpa Young's modulus and a final strength of 130 GPa, monolayer graphene is one of the strongest materials measured (11). For several years, zinc oxide nanostructures have been considered by researchers due to their low cost, easy access, biocompatibility and ease of surface modification due to different functional groups. Zinc oxide nanostructures have special physical and chemical properties, such as concentrated ultraviolet absorption or antimicrobial activity at pH in the range of 7 - 8, even in the absence of light. Therefore, they have wide applications in optical and antimicrobial devices (12). Zinc oxide has higher antimicrobial activity on the pathogen *Staphylococcus aureus* than other metal oxides. In addition, zinc oxide nanostructures are non-toxic and according to recent studies, these nanostructures do not cause degradation in the DNA of human cells (13).

2. Objectives

The aim of this study was to obtain a biodegradable nanostructure with antibacterial properties that can have the required mechanical properties of hard tissue and is also biodegradable. To achieve this goal, 9 composite nanostructures were fabricated. According to this goal in this study, the antibacterial behavior of PLA/PCL/HA nanocomposites containing zinc oxide and graphene was investigated and also the physical and biological properties of the samples were investigated and tested. Finally, the optimal sample was selected according to the results. This study will help to achieve absorbable orthopedic joints.

3. Methods

Polylactic acid with a molecular weight of 182,000 g/mol and polycaprolactone with a molecular weight of 80,000 g/mol were prepared by Sigma Aldrich. Graphene nanosheets with 2 - 8 nm thickness and purity of more than 95% were prepared from Sigma Aldrich. Zinc oxide nanoparticles with a purity of more than 99% and a particle size of 35 - 45 nm were prepared from Sigma Aldrich. Hydroxyapatite nanoparticles and FBS solution were prepared from Pardis Pajouhan Fanavaran Yazd Company.

Oleic acid and chloroform were obtained from Merck. *Escherichia coli* and *S. aureus* were used to perform photometric concentration measurement and zone of inhibition test, and fibroblast cells were used to evaluate the toxicity of nanostructures, all of which were obtained from the domestic market.

3.1. Fabrication of Polymer Scaffolds by Solution Method

To prepare nanocomposite samples, 40 g of polylactic acid and 10 g of polycaprolactone were first vacuumed at 80°C for 24 hours to dehumidify the granules. In this study, chloroform was selected as the solvent and suspending agent for nanoparticles. Nine samples were prepared for the preparation of pure and reinforced nanocomposites. To prepare a pure sample, 5 g of polylactic acid with 1.2 g of polycaprolactone was poured into 100 mL of chloroform. The mixture was stirred at 60°C for 6 hours to dissolve completely. The sample was then exposed to ultrasonic waves at a frequency of 45 kHz, at room temperature and with a power of 60 w. After 30 minutes, the sample was poured into a petri dish and placed under the hood to completely remove the solvent. To add 1 wt% of hydroxyapatite nanoparticles to the polymer matrix, first 0.062 g of hydroxyapatite nanoparticles in 10 ml of chloroform were placed on a stirrer for 10 minutes. Then oleic acid and chloroform with a ratio of 0.6% v/v was placed on the stirrer for 5 minutes at 70°C. The mixture was then added to a container containing polymers and solvents prepared in accordance with the sample. The sample was exposed to ultrasound for 30 minutes under similar conditions. The nanocomposite was then transferred to a petri dish and placed under the hood to remove the solvent.

3.1.1. Modification of Composite Scaffold with Zinc Oxide Nanoparticles

To make samples containing zinc oxide nanoparticles, 3 samples containing 0.1, 0.5 and 1 wt% of nanoparticles were added to the composite matrix. To make nanocomposites containing zinc oxide, the base matrix was prepared according to the steps mentioned above. After fabrication of the nanocomposite, 0.1% zinc oxide nanoparticles were poured into 10 cc of chloroform and irradiated with ultrasound for 15 minutes under the same conditions as other samples. After homogeneous dispersion of the nanoparticles in the solvent, the mixture was added to a polymer mixture containing hydroxyapatite. The sample was irradiated with ultrasound for 15 minutes in an ultrasonic bath. The sample was then transferred to a petri dish and placed under the hood for 48 hours to completely remove the solvent. The same steps were performed to make other weight percentages.

3.1.2. Modification of Composite Scaffolds with Graphene Nanosheets

The same process was repeated to make composite nanostructures containing graphene nanosheets. The weight percentages of graphene nanosheets added to the polymer matrix are 0.1, 0.5 and 1 wt%.

4. Results

4.1. Characterization of Composite Nanostructures

Field emission scanning electron microscopy (FESEM) method was used to study the morphology and distribution of nanoparticles in nanocomposites. In this study, Tescan VEGA II field emission scanning electron microscope was used. To confirm the presence of nanoparticles, X-ray diffraction spectroscopy (EDS) test was prepared from cross-section of PLA-PCL-HA-1% ZNO-1 Gr% nanocomposite. Also, to investigate the distribution of nanoparticles in the polymeric matrix, elemental analysis maps of the cross-section of the mentioned nanocomposite were prepared. As shown in Figure 1A - D, the surface of the nanocomposites is completely porous. The size of the pores on the surface was measured in the range of 1.5 to 3.5 μm. The porosities are uniformly observed on the surface of the nanocomposite and the size of the porosities is close to each other. A number of porosities are interconnected. The surface is free of cracks and fractures. By adding zinc oxide nanoparticles in the polymer matrix, bumps and white spots are observed on the surface, which indicates the presence of nanoparticles. By adding graphene nanosheets, the surface becomes more integrated and the porosity of the surface is reduced. Figure 2A-E and H shows cross-sectional images of composite nanostructures. As can be seen in the images, the nanoparticles of hydroxyapatite, zinc oxide and graphene are marked with yellow arrows in the image. Graphene nanosheets in the polymer matrix are seen as clear sheets in the polymer matrix. As you can see in the pictures, the graphene plates are fully open and have a good distribution. To investigate the presence of nanoparticles, X-ray energy diffraction (EDS) spectroscopy was performed at the same time as FESEM test. Its diagram is shown in Figure 3. As shown in Figure 3, the distribution of calcium, phosphorus and zinc oxide nanoparticles is shown in the elemental analysis map. Scattering of nanoparticles is well observed on the surface of composite nanostructures (14).

4.2. Investigation of Mechanical Properties

4.2.1. Bending Test

Equations 1, have been used to calculate the flexural properties under three-point loading and the modulus of elasticity.

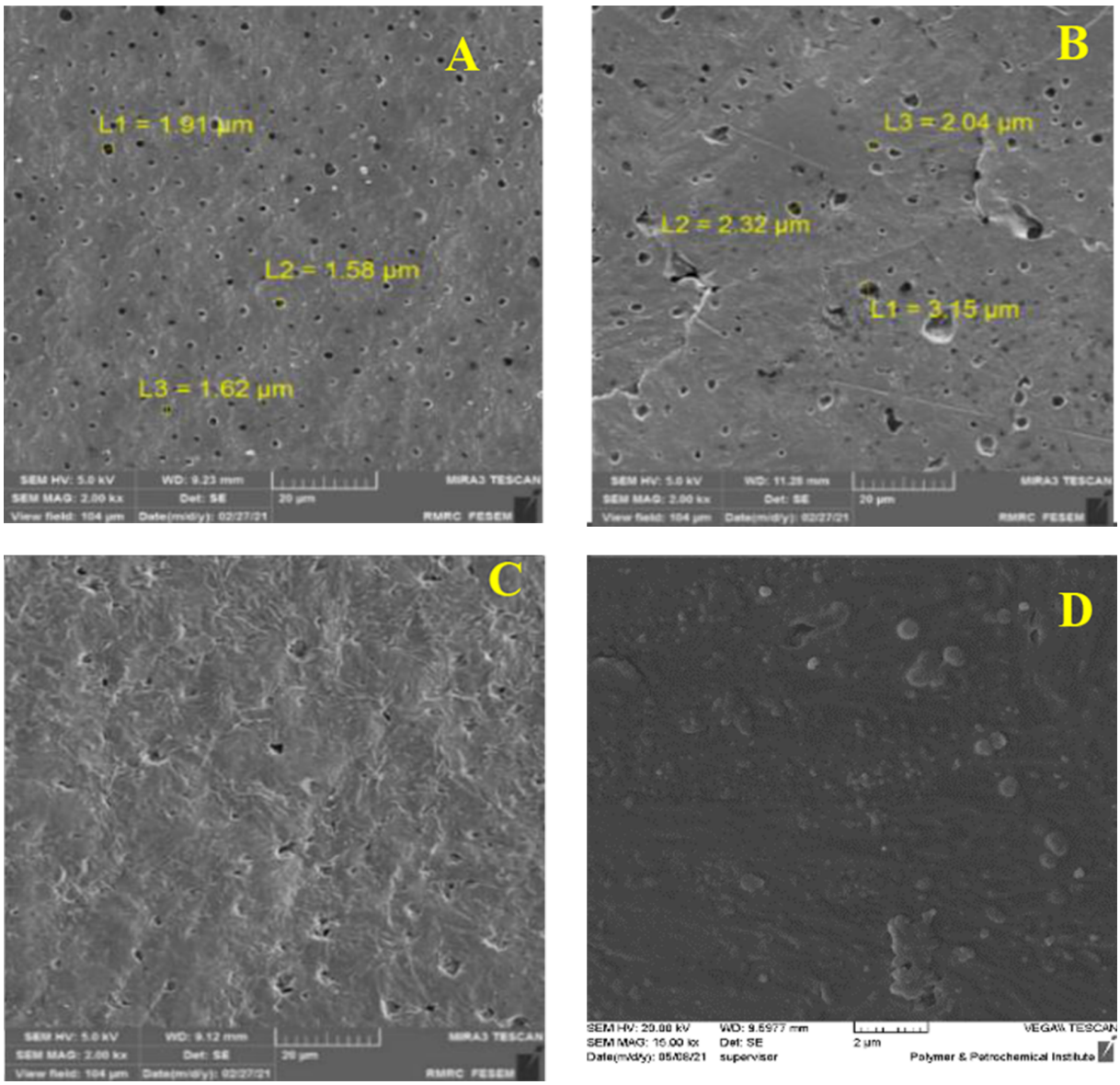

Figure 1. (A) PLA-PCL, (B) PLA-PCL-HA, (C) PLA-PCL-HA-1% ZNO, with magnification 2000 times, (D) PLAPCL-HA-1% ZNO-1% Gr with magnification 15000 times

$$\sigma_f = \frac{3FL}{2bd^2} \quad (1)$$

$$\epsilon_f = \frac{6bd}{l^2} \quad (2)$$

$$E = \frac{L^3}{4bd^3} \quad (3)$$

Where F represents the force, L is the length of the specimen between the two supports, b is the width of the specimen, is rectangular, and d is the thickness of the specimen. Where σ_f, ε_f and E are the flexural stress and strain and the Young's modulus, respectively. The calculated values before immersion in SBF solution are given in Table 1. Due to the similarity of the ions in SBF solution compared to human blood plasma and the creation of similar conditions when the implant was exposed to body fluids, the behavior of the composites in the bending test after immersion in SBF solution was performed and the calculated values after immersion in SBF solution are given in Table 2. The strain stress curves before and after immersion in the simulated body fluid are shown in Figures 4 and 5 (14, 15).

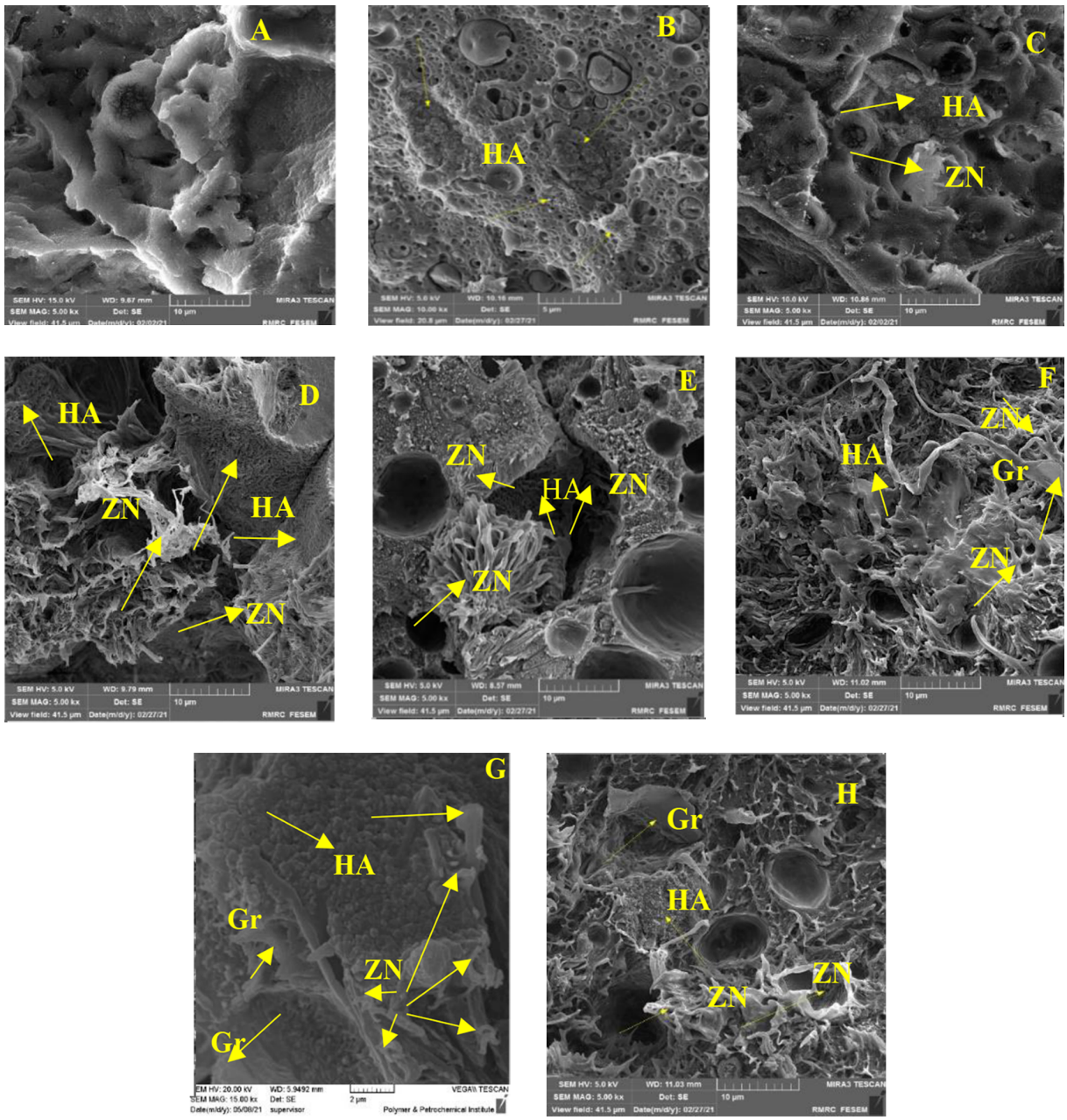

Figure 2. FESEM of cross section (A) PLA-PCL, (B) PLA-PCL-HA, (C) PLA-PCL-HA-0.1% ZNO, (D) PLA-PCLHA-0.5% ZNO, (E) PLA-PCL- HA1% ZNO, (F) PLA-PCL-HA-0.1% ZNO-0.1% Gr, (G) PLA-PCL-HA-0.5% ZNO-0.5% Gr, (H) PLA-PCL-HA-1% ZNO-1% Gr

Stress-strain curve of the bending test of composite nanostructures before and after immersion in SBF solution are shown in Figures 2 and 3, respectively.

4.3. Investigation of Bioactivity of Composite Nanostructures

In order to evaluate the bioactivity of the polymer matrix and composite nanostructures, the growth rate of apatite on the surface of the samples was investigated. If apatite grows on the surface of the samples, it can be said that the polymer matrix and the made nanocomposites are bioactive and can be placed in the host body and can stimulate bone formation. Also, by observing cracks on the surface of the polymer matrix and composite nanostructures, the beginning of the degradation process of the samples

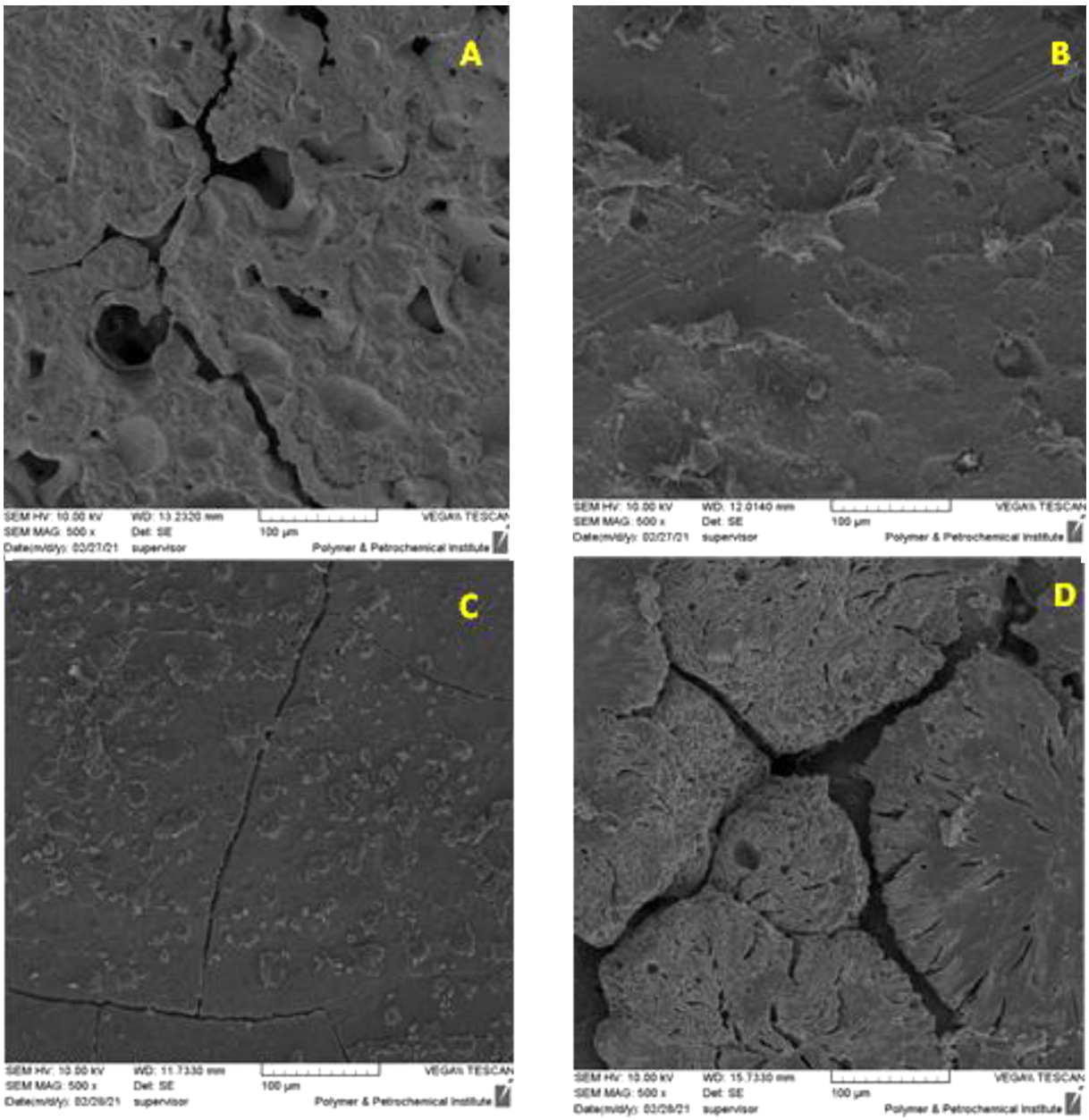

Figure 3. FESEM of nanocomposite degradation process and apatite growth on the surface (A) PLA-PCL polymer matrix, (B) PLA-PCL-HA, (C) PLA-PCL-HA-1% ZNO, (D) PLA-PCL-HA-1% ZNO-1% Gr with 500x magnification

was determined. To investigate this issue, FESEM images of the samples were examined after 1 month of immersion in (SBF). The results are shown in Figure 6 (15).

4.4. Biodegradability Test

To evaluate the biodegradability, parts of each sample were cut. The pieces were weighed by a scale of 4 decimal places. Each piece was placed in a 15 mL Falcon. The Falcons were filled with SBF and placed in a water bath on a stirrer at room temperature. To measure the weight of the samples in the dry state, the samples were washed immediately after leaving the SBF solution with a sufficient amount of deionized water and dried at room temperature for 48 hours and then weighed. The results are shown in Figure 7. As shown in Figure 7, no weight loss was observed

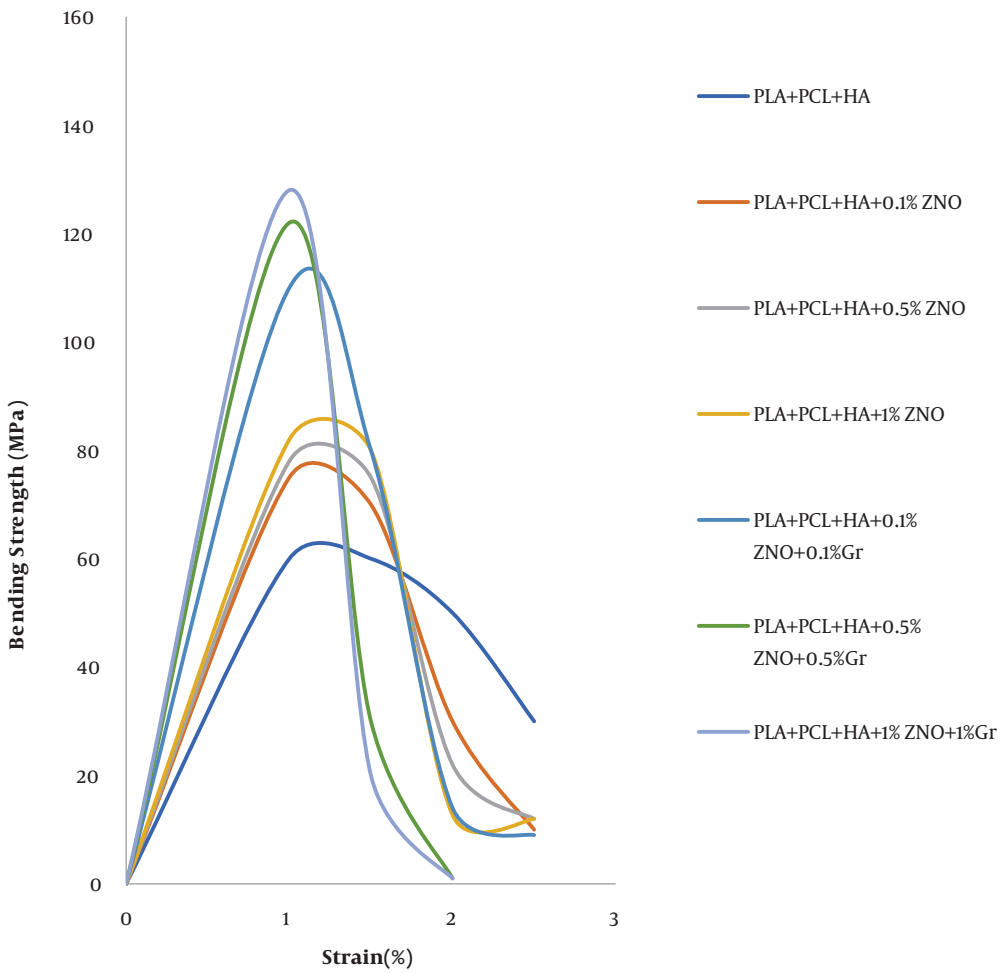

Figure 4. Stress-strain curve of bending test of nanocomposite samples before immersion in SBF solution

Table 1. Results of Bending Test of Nanocomposites Before Immersion in SBF Solution

Sample	Young's Flexural (MPa) Modulus	Probability
PLA-PCL-HA	2352.94 ± 138.261	0.017
PLA-PCL-HA-0.1%ZNO	3336.898 ± 276.349	0.015
PLA-PCL-HA-0.5%ZNO	312.833 ± 3337.679	0.013
PLA-PCL-HA-1%ZNO	3508.021 ± 378.126	0.008
PLA-PCL-HA-0.1%ZNO-0.1%Gr	4705.882 ± 426.769	0.005 >
PLA-PCL-HA-0.5ZNO-0.5%Gr	5219.251 ± 467.924	0.005 >
PLA-PCL-HA-1%ZNO-1%Gr	5475.935 ± 520.489	0.005 >

Table 2. Calculated Values of Bending Test of Composite Nanostructures After 15 Days of Immersion in SBF Solution

Sample	Young's Flexural (MPa) Modulus	Probability
PLA-PCL-HA	2139.037 ± 381.312	0.021
PLA-PCL-HA-0.1%ZNO	2652.406 ± 294.347	0.019
PLA-PCL-HA-0.5%ZNO	2737.967 ± 129.368	0.016
PLA-PCL-HA-1%ZNO	2994.652 ± 403.385	0.012
PLA-PCL-HA-0.1%ZNO-0.1%Gr	3850.267 ± 167.411	0.007
PLA-PCL-HA-0.5%ZNO-0.5%Gr	4064.171 ± 498.472	< 0.005
PLA-PCL-HA-1%ZNO-1%Gr	4363.636 ± 127.498	< 0.005

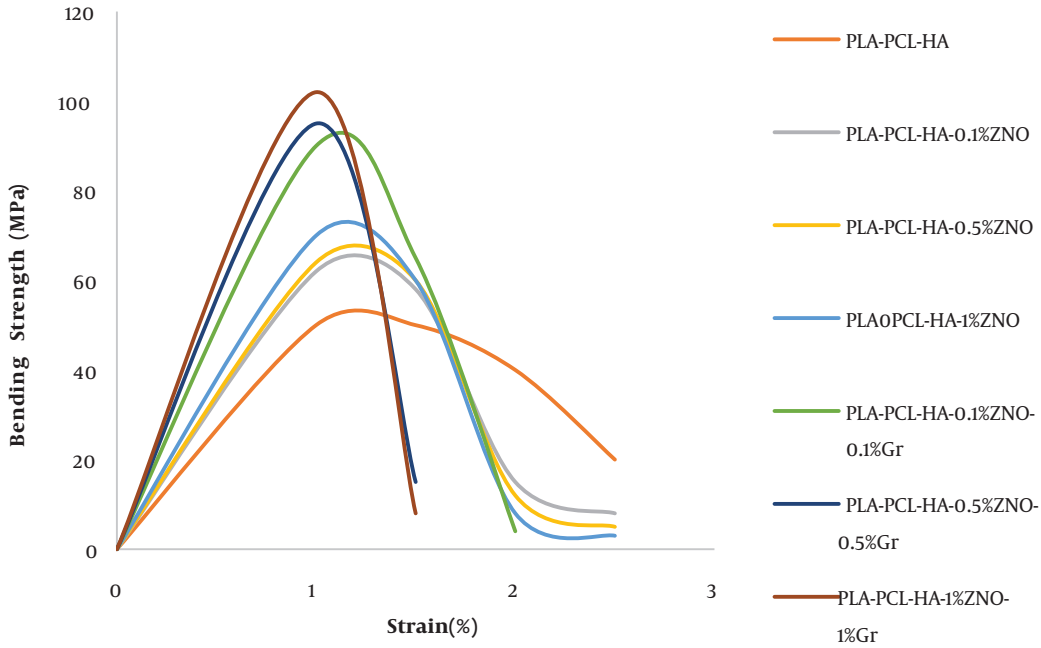

Figure 5. Stress-strain curve of bending test of nanocomposite samples after immersion in SBF solution

in the first week. From the second week onwards, the specimens began to lose weight with a gentle slope on the 1000th gram scale. From the tenth to the twentieth week, the weight loss rate accelerated slightly, indicating the destruction of polymer chains and the adsorption of the polymer matrix in the simulated body solution. The rate of weight loss in the samples is almost the same. In nanocomposites containing hydroxyapatite, with the beginning of the degradation and weight loss process, the growth of apatite takes place on the surface of the nanocomposite, and this affects the rate of weight loss on the scale of one thousandth of a gram. In samples containing oxidized nanoparticles, it is faster than the polymer matrix due to the release of ions on the degradation process with a very gentle slope. Graphene-containing nanocomposites have a similar rate of degradation process as other nanocomposites. Nanostructures containing hydroxyapatite are not expected to show a weight loss rate due to the apatite coating on the nanocomposite surface. But the weight loss process of these nanostructures continued. But the weight loss process of these nanostructures continued. After mixing HA in PLA/PCL nanocomposite, the degradation rate increased due to improved membrane hydrophilicity. It should be noted that the degradation rate of pure polymer matrix such as PLA/PCL as a control sample can be used to observe the positive effect of HA compound on nanocomposites because the nanocomposite had lost approximately 6.48% of its weight in 20 weeks. After careful evaluation of PLA-PCL-HA-1% ZNO and PLA-PCL-HA-1% ZNO-1% Gr nanocomposites, in vitro degradation of nanocomposites after the end of the period was about 8.92 and 9.31 increased, respectively. Percentage increased. It can be concluded that nanocomposites showed a continuous and higher biodegradation rate than PLA/PCL membrane (15, 16).

4.5. Toxicity Test

To evaluate the biocompatibility and cytotoxicity of the polymer matrix and the optimal nanostructure, the viability of L929 fibroblast cells in the presence of the polymer matrix and the optimal composite nanostructure was investigated. The results are shown as the percentage of L929 fibroblast cell survival after 1 day and 3 days in Table 3 and inverted light microscope images after 24 hours in Figure 8. The percentage of cell viability was calculated from Equation 4.

$$Cell\ viability\ (\%) = \frac{OD_{Sample}}{OD_{Control}} \times 100 \quad (4)$$

Examination of cell survival results shows that the cell survival rate in the vicinity of the optimal composite matrix after 24 hours was 84.96 ± 1.006% and with the passage of time up to 72 hours this rate decreased to 82.96 ± 1.101%.

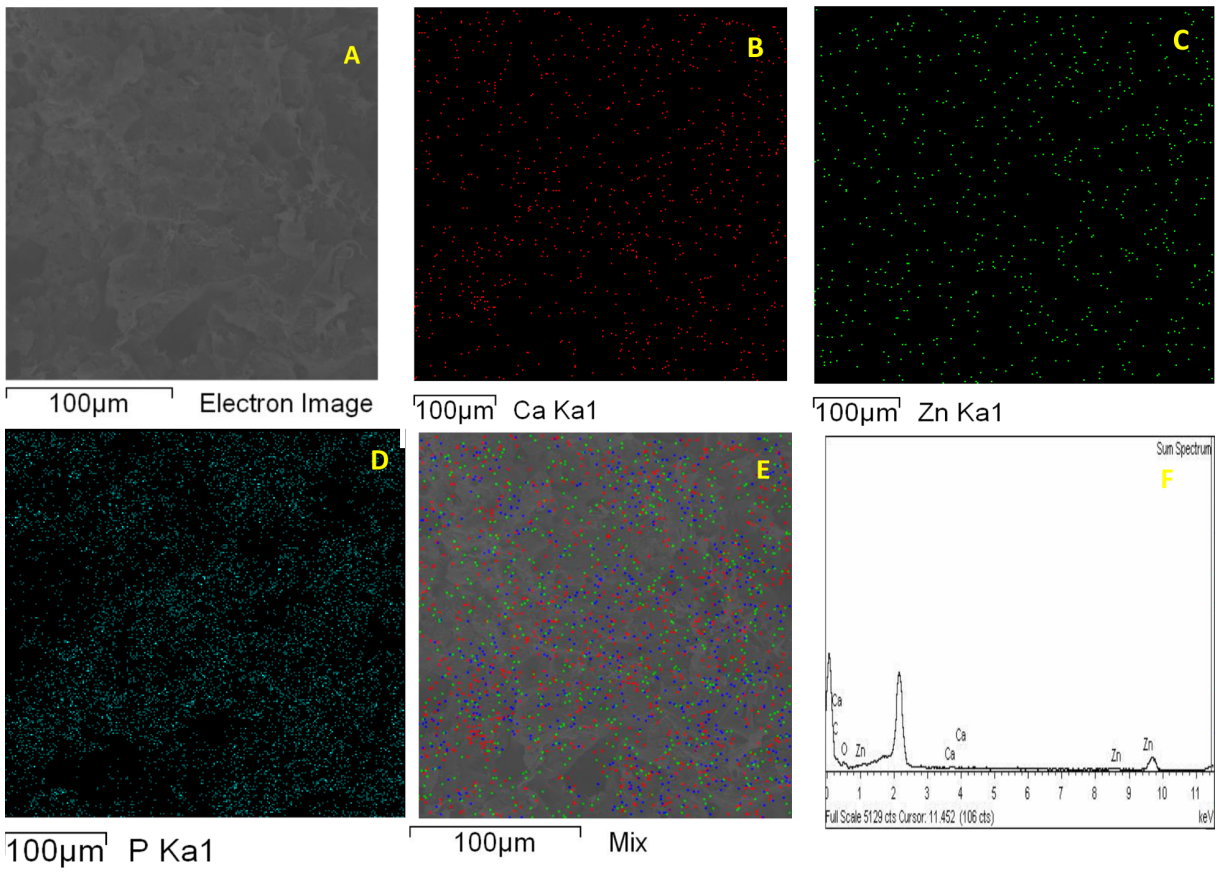

Figure 6. (A) FESEM image of cross section of PLA-PCL-HA-1% ZNO-1% Gr nanocomposite, elemental analysis map images of ion distribution (B) calcium, (C) zinc, (D) phosphorus, (E) mix of nanoparticles, and (F) spectrum X-ray energy diffraction measurement of nanocomposite cross-section

Table 3. Percentage of L929 Cell Viability in the Presence of Optimal Polymer Matrix and Composite Nanostructure After 24 and 72 Hours

Sample	Survival Rate After 24 Hours	Survival Rate After 72 Hours	Probability
PLA-PCL	25.82 ± 0.782	22.14 ± 0.623	< 0.005
PLA-PCL-HA-1% ZNO-1%Gr	84.96 ± 1.006	82.96 ± 1.101	< 0.005

The survival rate of cells against polymer matrix was25.82 ± 0.782% after 24 hours and 22.14 ± 0.623% after 72 hours. Cell viability in the presence of optimal composite shows a significant increase due to surface modification and improvement of surface properties and the positive effect of the presence of nanoparticles in the polymer matrix (17-20).

4.5. Zone of Inhibition Test

In order to investigate the antibacterial properties of the polymer matrix and the optimal composite nanostructure, the Zone of Inhibition test was performed. Gram-positive and gram-negative bacteria of *S. aureus* and *E. coli* were used for this purpose. As can be seen in the images, in the PLA-PCL polymer matrix sample, no growth inhibition zone is formed around the polymer matrix. Of course, no bacterial colonies are observed on the surface of the polymer matrix, which indicates the proper structure of the matrix. In the optimal sample, due to the presence of oxidized nanoparticles and graphene, the growth inhibition zone is clearly observed. The sharp edges of graphene nanosheets also cause the bacterial membrane to rupture, and resulting in bacterial death. The growth inhibition zone of *E. coli* is slightly lower than that of *S. aureus*, which is due to the structure of the membrane of the two layers of gram-negative bacteria against the monolayer wall of gram-positive bacteria. The images of the zone of inhibition of the optimal nanocomposite and polymer matrix are given in Figure 9. These results are consistent with the results of previous research. The antibacterial activity of

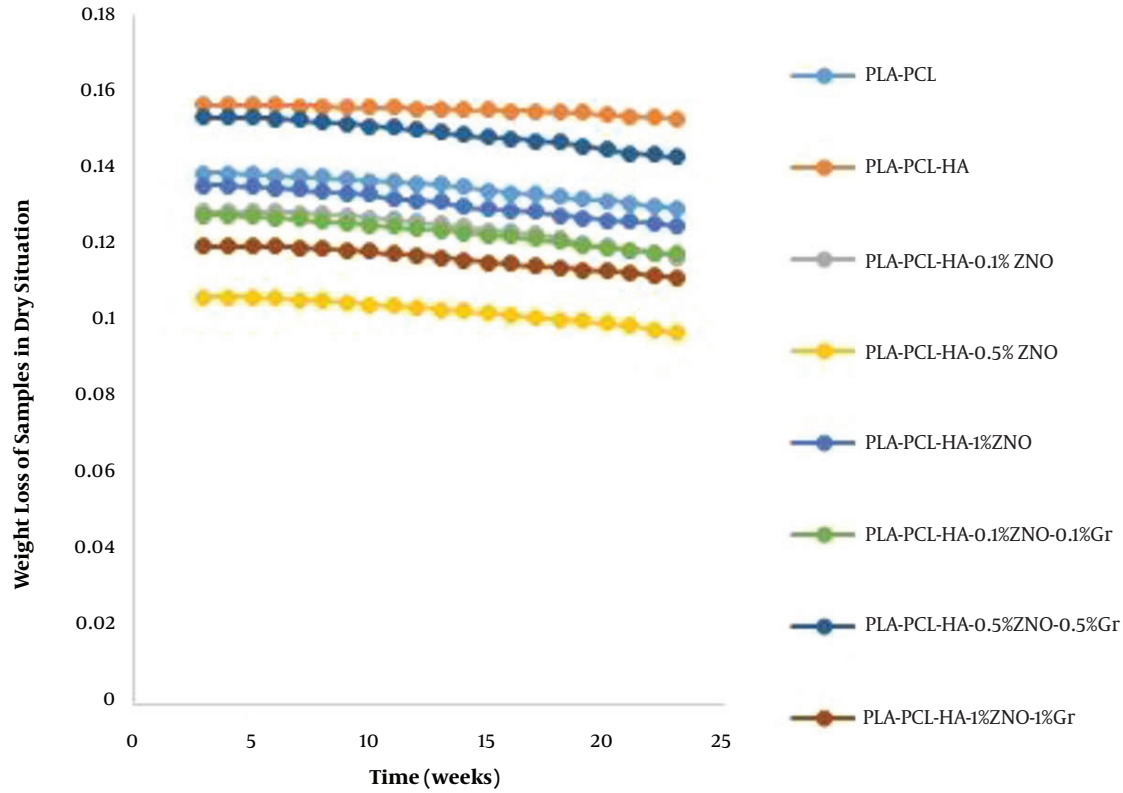

Figure 7. Weight loss diagram of polymer matrix and composite nanostructures weighed in dry situation

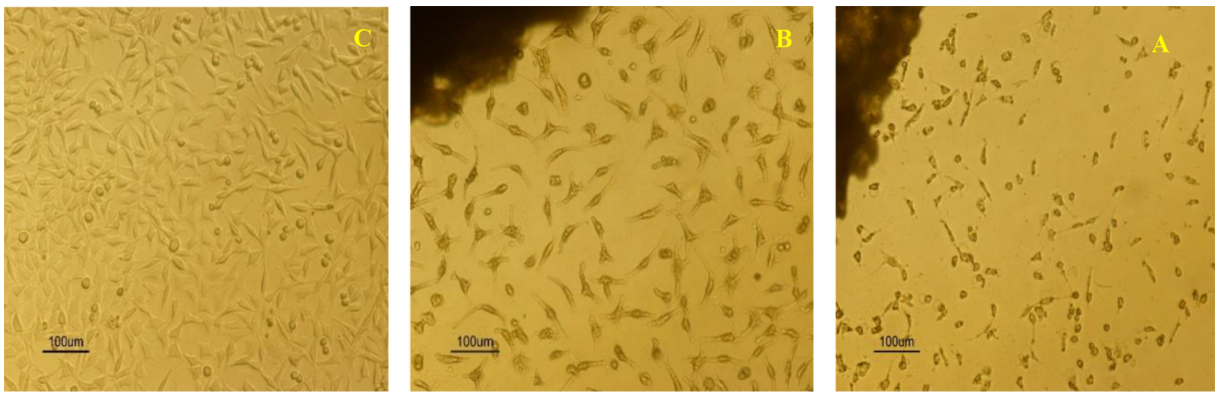

Figure 8. Inverted light microscope image of (A) polymeric matrix, (B) optimal matrix PLA-PCL-HA-1% ZNO-1% Gr, (C) control sample

nanocomposites not only involves the direct action of zinc oxide nanoparticles, but is also enhanced by the mechanism of release of zinc ions as well as the production of reactive oxygen species (ROS). In addition, graphene is the storage site for zinc ions, which are released from zinc oxide nanoparticles and, by contact with negative bacteria, increase the permeability of cells, which ultimately causes cell deformation and then leakage. Graphene can also improve the electron transfer rate due to its unique structure, which makes this nanocomposite have higher antibacterial activity (21, 22).

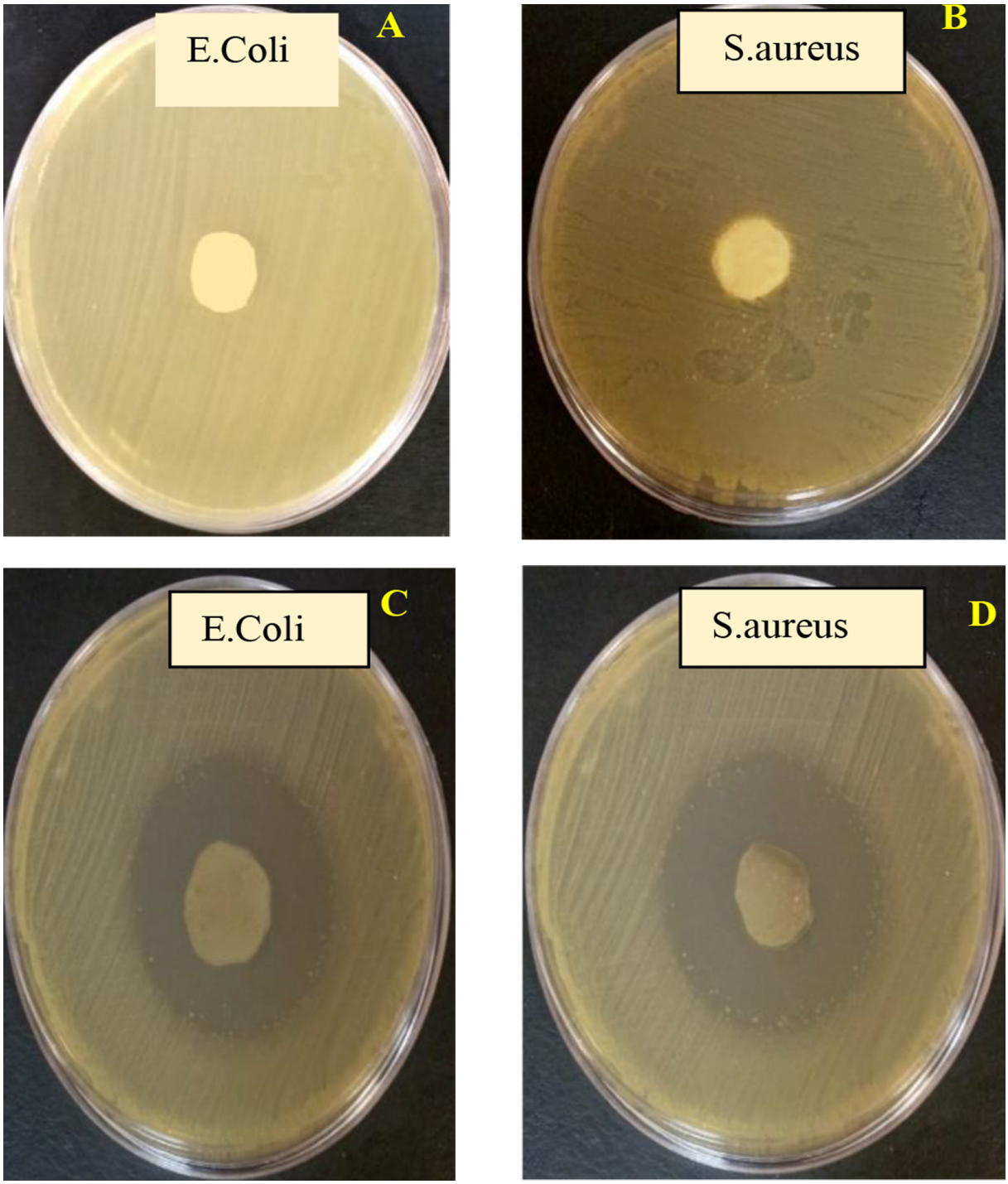

Figure 9. Images of zone of inhibition of polymeric matrix against (A) *Escherichia coli*, (B) *Staphylococcus aureus*, optimal nanocomposite zone of inhibition against (C) *E. coli*, (D) *S. aureus*

Table 4. Results of Photometric Concentration Test of PLA-PCL, PLA-PCL-HA-1% ZNO-1% Gr Against *Staphylococcus aureus* and *Escherichia coli*

Sample	Antibacterial Percentage of the Sample Against *Escherichia coli*	Antibacterial Percentage of the Sample Against *Staphylococcus aureus*	Probability
PLA-PCL	25.16 ± 0.209%	%27.14 ± 0.218	< 0.005
PLA-PCL-HA-1% ZNO-1%Gr	%76.87 ± 0.249	%79.17 ± 0.320	< 0.005

4.6. Photometric Concentration Measurement Test

To measure the antibacterial percentage of the samples, photometric concentration was measured on two samples of polymer matrix and optimal sample. The mortality rate was calculated from Equation 5. The results are given in Table 4.

$$mortality\ rate = 1 - \left[\left(\frac{Absorption\ of\ treatment\ samples}{Absorption\ of\ control\ samples}\right)\right] \times 100 \quad (5)$$

As shown in Table 4, the antibacterial content of the optimal sample against the polymeric matrix has almost tripled, that resulting in the release of zinc ions from the nanocomposite surface as well as the presence of graphene nanosheets. The result of this test is also consistent with the result of the zone of inhibition test (21, 22).

5. Discussion

In a study by Pietrzykowska et al., The flexural Young's modulus of pure polylactic acid was 1603 ± 175 MPa (23). While with adding HA nanoparticle to polymeric matrix flexural Young's modulus increased to 8104 ± 38 MPa (23). In a study conducted by Sadudeethanakul et al., the flexural strength of polylactic acid-hydroxyapatite nanocomposite was investigated. It was found that the best result was obtained by adding 5% hydroxyapatite (24). In a study by Ko et al., the flexural modulus of polylactic acid nanocomposites containing hydroxyapatite was reduced compared to pure polylactic acid, because the interfacial adhesion was not sufficiently improved (25). In this study, the addition of nanoparticles also improved the flexural modulus. The addition of graphene and zinc oxide nanoparticles also improved the antibacterial properties of the optimal sample against the control sample. The results of this study are consistent with the results of research conducted by other researchers.

5.1. Conclusions

The composite nanostructure is biodegradable, so there is no need for re-surgery to remove the implant from the body after repair. The flexural Yang modulus of the PLA-PCL-HA nanocomposite was 2139.037 ± 381.312 MPa. The presence of zinc oxide and graphene nanoparticles increased the Young's modulus to 4363.636 ± 127.498 MPa. The Young's modulus of the optimal sample close to the Young's modulus of spongy bone. Due to the biodegradability of the implant and due to the temporary presence of the implant in the body tissue, it will cause a minimal immune response. Also, due to the antibacterial properties of the nanocomposite, the patient needs to take antibiotics is reduced. Therefore, this nanocomposite has sufficient potential for use in orthopedic surgeries in spongy bone.

Acknowledgments

Thanks to everyone who helped us with this research.

Footnotes

Authors' Contribution: Study concept and design, F. D. F., A. R. S., A. A.; acquisition of data, F. D. F.; analysis and interpretation of data, F. D. F., A. R. S., A. A.; drafting of the manuscript, F. D. F.; critical revision of the manuscript for important intellectual content, A. R. S., A. A.; statistical analysis, F. D. F.; administrative, technical, and material support, A. R. S., F. D. F., A. A.; study supervision, A. R. S., A. A.

Conflict of Interests: It was not declared by the author.

Funding/Support: There is no funding/support.

References

1. Kim HW, Lee HH, Knowles JC. Electrospinning biomedical nanocomposite fibers of hydroxyapatite/poly(lactic acid) for bone regeneration. *J Biomed Mater Res A*. 2006;**79**(3):643–9. [PubMed ID: 16826596]. https://doi.org/10.1002/jbm.a.30866.
2. Gong M, Zhao Q, Dai L, Li Y, Jiang T. Fabrication of polylactic acid/hydroxyapatite/graphene oxide composite and their thermal stability, hydrophobic and mechanical properties. *Journal of Asian Ceramic Societies*. 2018;**5**(2):160–8. https://doi.org/10.1016/j.jascer.2017.04.001.
3. Causa F, Netti PA, Ambrosio L, Ciapetti G, Baldini N, Pagani S, et al. Poly-epsilon-caprolactone/hydroxyapatite composites for bone regeneration: in vitro characterization and human osteoblast response. *J Biomed Mater Res A*. 2006;**76**(1):151–62. [PubMed ID: 16258959]. https://doi.org/10.1002/jbm.a.30528.
4. Wang G, He C, Yang W, Qi F, Qian G, Peng S, et al. Surface-Modified Graphene Oxide with Compatible Interface Enhances Poly-L-Lactic Acid Bone Scaffold. *J Nanomater*. 2020;**2020**:1–11. https://doi.org/10.1155/2020/5634096.

5. Madhavan Nampoothiri K, Nair NR, John RP. An overview of the recent developments in polylactide (PLA) research. *Bioresour Technol*. 2010;**101**(22):8493–501. [PubMed ID: 20630747]. https://doi.org/10.1016/j.biortech.2010.05.092.
6. Abedalwafa M, Wang F, Wang L, Li C. Biodegradable poly-epsilon-caprolactone (PCL) for tissue engineering applications: a review. *Rev. Adv. Mater. Sci*. 2013;**34**(2):123–40.
7. Russias J, Saiz E, Nalla RK, Gryn K, Ritchie RO, Tomsia AP. Fabrication and mechanical properties of PLA/HA composites: A study of in vitro degradation. *Mater Sci Eng C Biomim Supramol Syst*. 2006;**26**(8):1289–95. [PubMed ID: 26301264]. [PubMed Central ID: PMC4544836]. https://doi.org/10.1016/j.msec.2005.08.004.
8. Li J, Lu XL, Zheng YF. Effect of surface modified hydroxyapatite on the tensile property improvement of HA/PLA composite. *Appl Surf Sci*. 2008;**255**(2):494–7. https://doi.org/10.1016/j.apsusc.2008.06.067.
9. Wan C, Chen B. Reinforcement and interphase of polymer/graphene oxide nanocomposites. *J Mater Chem A*. 2012;**22**(8):3637. https://doi.org/10.1039/c2jm15062j.
10. Scaffaro R, Botta L, Maio A, Mistretta MC, La Mantia FP. Effect of Graphene Nanoplatelets on the Physical and Antimicrobial Properties of Biopolymer-Based Nanocomposites. *Materials (Basel)*. 2016;**9**(5). [PubMed ID: 28773475]. [PubMed Central ID: PMC5503009]. https://doi.org/10.3390/ma9050351.
11. Therias S, Larche JF, Bussiere PO, Gardette JL, Murariu M, Dubois P. Photochemical behavior of polylactide/ZnO nanocomposite films. *Biomacromolecules*. 2012;**13**(10):3283–91. [PubMed ID: 22967047]. https://doi.org/10.1021/bm301071w.
12. Sawai J. Quantitative evaluation of antibacterial activities of metallic oxide powders (ZnO, MgO and CaO) by conductimetric assay. *J Microbiol Methods*. 2003;**54**(2):177–82. [PubMed ID: 12782373]. https://doi.org/10.1016/s0167-7012(03)00037-x.
13. Wu D, Samanta A, Srivastava RK, Hakkarainen M. Starch-Derived Nanographene Oxide Paves the Way for Electrospinnable and Bioactive Starch Scaffolds for Bone Tissue Engineering. *Biomacromolecules*. 2017;**18**(5):1582–91. [PubMed ID: 28350456]. https://doi.org/10.1021/acs.biomac.7b00195.
14. Chen C, Sun X, Pan W, Hou Y, Liu R, Jiang X, et al. Graphene Oxide-Templated Synthesis of Hydroxyapatite Nanowhiskers To Improve the Mechanical and Osteoblastic Performance of Poly(lactic acid) for Bone Tissue Regeneration. *ACS Sustain Chem Eng*. 2018;**6**(3):3862–9. https://doi.org/10.1021/acssuschemeng.7b04192.
15. Rezgui F, Swistek M, Hiver JM, G'Sell C, Sadoun T. Deformation and damage upon stretching of degradable polymers (PLA and PCL). *Polymer*. 2005;**46**(18):7370–85. https://doi.org/10.1016/j.polymer.2005.03.116.
16. Davoodi S, Oliaei E, Davachi SM, Hejazi I, Seyfi J, Heidari B, et al. Preparation and characterization of interface-modified PLA/starch/PCL ternary blends using PLLA/triclosan antibacterial nanoparticles for medical applications. *RSC Adv*. 2016;**6**(46):39870–82. https://doi.org/10.1039/c6ra07667j.
17. Özge Erdohan Z, Çam B, Turhan KN. Characterization of antimicrobial polylactic acid based films. *J Food Eng*. 2013;**119**(2):308–15. https://doi.org/10.1016/j.jfoodeng.2013.05.043.
18. Emami-Karvani Z. Antibacterial activity of ZnO nanoparticle on Gram-positive and Gram-negative bacteria. *Afr J Microbiol Res*. 2012;**5**(18). https://doi.org/10.5897/ajmr10.159.
19. Brown A, Zaky S, Ray H, Sfeir C. Porous magnesium/PLGA composite scaffolds for enhanced bone regeneration following tooth extraction. *Acta Biomater*. 2015;**11**:543–53. [PubMed ID: 25234156]. https://doi.org/10.1016/j.actbio.2014.09.008.
20. O'Connor JP, Kanjilal D, Teitelbaum M, Lin SS, Cottrell JA. Zinc as a Therapeutic Agent in Bone Regeneration. *Materials (Basel)*. 2020;**13**(10). [PubMed ID: 32408474]. [PubMed Central ID: PMC7287917]. https://doi.org/10.3390/ma13102211.
21. Wang YW, Cao A, Jiang Y, Zhang X, Liu JH, Liu Y, et al. Superior antibacterial activity of zinc oxide/graphene oxide composites originating from high zinc concentration localized around bacteria. *ACS Appl Mater Interfaces*. 2014;**6**(4):2791–8. [PubMed ID: 24495147]. https://doi.org/10.1021/am4053317.
22. El-Shafai N, El-Khouly ME, El-Kemary M, Ramadan M, Eldesoukey I, Masoud M. Graphene oxide decorated with zinc oxide nanoflower, silver and titanium dioxide nanoparticles: fabrication, characterization, DNA interaction, and antibacterial activity. *RSC Adv*. 2019;**9**(7):3704–14. [PubMed ID: 35518070]. [PubMed Central ID: PMC9060286]. https://doi.org/10.1039/c8ra09788g.
23. Pietrzykowska E, Romelczyk-Baishya B, Chodara A, Koltsov I, Smogor H, Mizeracki J, et al. Microstructure and Mechanical Properties of Inverse Nanocomposite Made from Polylactide and Hydroxyapatite Nanoparticles. *Materials (Basel)*. 2021;**15**(1). [PubMed ID: 35009328]. [PubMed Central ID: PMC8745816]. https://doi.org/10.3390/ma15010184.
24. Sadudeethanakul S, Wattanutchariya W, Nakkiew W, Chaijaruwanich A, Pitjamit S. Bending strength and Biological properties of PLA-HA composites for femoral canine bone fixation plate. *IOP Conf Ser Mater Sci Eng*. 2019;**635**(1):12004. https://doi.org/10.1088/1757-899x/635/1/012004.
25. Ko HS, Lee S, Lee D, Jho JY. Mechanical Properties and Bioactivity of Poly(Lactic Acid) Composites Containing Poly(Glycolic Acid) Fiber and Hydroxyapatite Particles. *Nanomaterials (Basel)*. 2021;**11**(1). [PubMed ID: 33477735]. [PubMed Central ID: PMC7832325]. https://doi.org/10.3390/nano11010249.